

Deuteration Effects on the Enthalpy and Entropy Changes in Encapsulation of the Methyl-containing Guest Molecules in Molecular Cage: Importance of Increase of the Internal Rotation Barrier

Suehiro IWATA* and Takaharu HAINO**

The reported isotope effects on the enthalpy ΔH_{encaps}^{VH} and entropy ΔS_{encaps}^{VH} changes in the encapsulation equilibrium were analyzed by assuming the increase of the barrier height of the end methyl groups of a guest molecule inside of the self-assembled molecular cage. Haino et al (Reference¹⁾) found exceptionally large deuteration effects in the ratio of equilibrium constants, K_D^{eq}/K_H^{eq} , and its temperature dependence for the guest encapsulation reaction in the self-assembled molecular cage. All of the guest molecules have a methyl group at both end of the molecule. They determined the changes of the enthalpy ΔH_{encaps}^{VH} and entropy ΔS_{encaps}^{VH} by replacing the CH_3 with the CD_3 of both ends of the guest molecule, and the enormously large effects were found. The observed large negative changes in $\Delta_{D-H}\Delta H_{encaps}^{VH}$ and $\Delta_{D-H}\Delta S_{encaps}^{VH}$ are semi-quantitatively explained by assuming that the barrier height of the internal rotation of the methyl groups increases by the encapsulation, which indirectly proves that the end methyl groups of the guest molecule are non-covalently interacted with the aromatic rings of the host cage.

INTRODUCTION

Metal-coordination driven self-assembly is now used to create a variety of multi-component self-assemblies. In particular, to generate supramolecular architecture having nanometric cavities, the metal-coordination driven self-assemblies are being developed intensively²⁾. Among them, the cavitand-based coordination capsules and cages have received a great deal of attention because of their unique guest-binding property inside of the cavity. By introducing four ligation sites, such as pyridyl, nitrile and dithiocarbamate, on the upper rim of the cavitands, tetradentate ligands are provided, and these ligands assemble through the metal coordination to form a capsule or a cage³⁾. Adopting these strategy, Haino and his coworkers succeeded in synthesizing a new self-assembling capsule in which two octadentate cavitands, having four bipyridyl groups each, coordinate to four silver cations in a tetrahedral way⁴⁾. Recently they extended the work to synthesize another new capsule of nano size, and demonstrated that the capsule can be a size- and shape-selective host for some organic molecules⁵⁾. They established the necessary condition that a guest molecule is encapsulated in the new host molecule. One of the conditions is that the guest molecule has a methyl group at both ends, which are interacted non-covalently with the aromatic rings of the capsule. Furthermore, by monitoring the signal intensity of the NMR, the equilibrium constants K_{encaps} of the encapsulation reactions for several guest molecules were determined at several temperatures, and then from the slope and the intercept of the Van't Hoff plots, the effective enthalpy change ΔH_{encaps}^{VH} and entropy change ΔS_{encaps}^{VH} in the encapsulation reactions were reported⁵⁾. They successfully extended the works to synthesize the guest molecules having the deuterated methyl groups. Furthermore they determined the deuterated effects on the effective enthalpy change ΔH_{encaps}^{VH} and entropy change ΔS_{encaps}^{VH} by using the the competition

2009年2月2日受理

* 豊田理化学研究所フェロー

** 広島大学大学院理学研究科

equilibrium between the protiated and deuterated guest molecules in the encapsulation reactions⁶⁾, and found the enormous large changes $\Delta_{D-H}\Delta H_{encaps}^{VH}$ and $\Delta_{D-H}\Delta S_{encaps}^{VH}$ both in the slope and intercept of the Van't Hoff plots. In next section the experimental findings on the deuteration effects of the thermochemical properties in the encapsulation reaction are briefly reviewed. Because the observed large changes in the thermochemical properties by the deuteration cannot be explained with the normal isotope effects caused by the change of the C-H(D) vibrational frequencies, in the following section, we postulate that the increase of the methyl rotation barrier by the encapsulation is responsible for the observed isotope effects. The quantum levels of the internal rotation of a methyl group are sensitive both to the inertia moment of the methyl group and to the barrier height of the internal rotation, and thus, if the barrier height of the methyl group is increased by the local molecular interaction inside of the host cage, it is expected that the chemical equilibrium of the encapsulation is affected by the deuteration of the methyl hydrogens. Some simple numerical calculations demonstrate that this model can qualitatively and semi-quantitatively explain the observed effects. The thermochemical properties of the chemical equilibrium in the encapsulation reaction are strongly related to the molecular interaction between the host and guest molecules and to the dynamic motion of the guest molecule inside of the capsule. Therefore, the qualitative elucidation of the observed isotope effects helps to understand the characteristics of the guest encapsulation in the self-assembled molecular cage.

A SHORT SUMMARY OF THE EXPERIMENTAL FINDINGS

A nano capsule Haino and his coworkers synthesized and used as a host molecule is **1** in Figure 1 with four counter anion BF_4^- ⁵⁾.

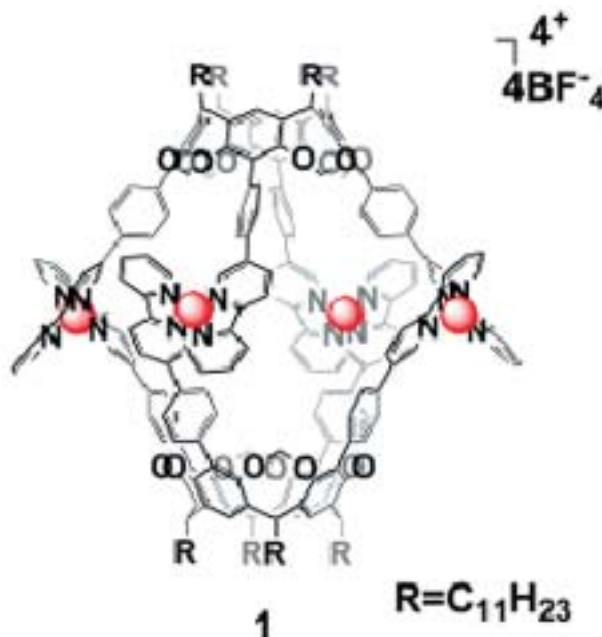


Figure 1. The self-assembled host molecule. The spheres surrounded by four nitrogen atoms are the Ag ions.

The host molecule consists of two equivalent cavitands ($2 = [(\text{C}_5\text{H}_4\text{N}-\text{C}_5\text{H}_3\text{N}-\text{C}_6\text{H}_4-\text{C}_6\text{H}_1(\text{OCH}_2\text{O})_2\text{CH}_2\text{R})_4$, $R = \text{C}_{11}\text{H}_{23}$) and four silver cations Ag^+ ; the ion pair is $[(2)_2\text{Ag}_4^+(\text{BF}_4)_4^-]$. By connected with the silver ions, two cavitands create a huge space inside of the metal complex. The ^1H NMR spectrum in CD_3Cl showed that the eight bipyridyl groups are magnetically equivalent, and that the metal complex is chiral in D_4 symmetry. In the molecular model created with MacroModel V6.5⁷⁾ using the Amber force field, the estimated distance from the bottom of one cavitand to the other is about 16Å and the estimated volume of the cavity is about 580Å³. In contrast to the huge size of the hollow in the metal complex **1**, a single cavitand **2** itself has a

rather small bowl at the bottom, which allows to contain a methyl group whose hydrogen atoms interact with the π rings of the phenyls. These characteristics of the structure of the capsule suggest that the capsule can encapsulate a guest molecule which should be in an appropriate length of a cylindrical form to fit to the cavity. In addition, a guest molecule might be preferable to have a methyl group at both ends or at least one end of the molecule, to induce the weak attractive interaction between C-H of the methyl and the π rings of the phenyls⁸.

Haino and his coworkers designed and synthesized a series of guest molecules⁵. Some of the representatives are shown in Figure 2.

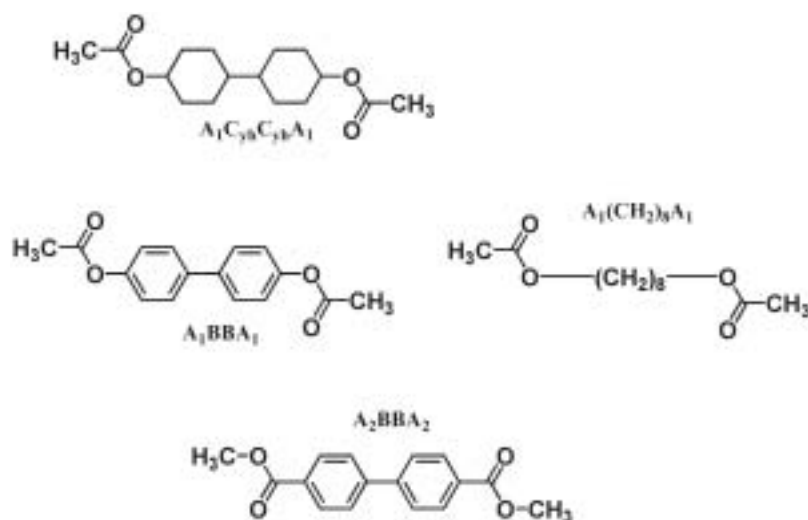


Figure 2. The guest molecules studied by Haino et al⁵.

By changing the concentration of the guest molecules, they determined the equilibrium constant K^{eq} for the encapsulation equilibrium



monitoring the NMR signal intensity of the hydrogens of methyl groups, where A stands for the host molecule and $\mathbf{G}(\text{CH}_3)$ stands for a guest molecule having a protiated methyl at both ends of the molecule. By measuring K^{eq} at several temperatures, from the Van't Hoff plot

$$\ln K_{\text{H}}^{eq} = -\frac{\Delta G_{\text{encaps}}}{RT} = -\frac{\Delta H_{\text{encaps}}^{VH}}{RT} + \Delta S_{\text{encaps}}^{VH} \quad (2)$$

the slope $\Delta H_{\text{encaps}}^{VH}$ and the intercept $\Delta S_{\text{encaps}}^{VH}$ are determined. They are summarized in Table 1⁵. For guests A_1BBA_1 and $\text{A}_1\text{C}_{7a}\text{C}_{7b}\text{A}_1$, the extremely large equilibrium constant at room temperature and the large effective enthalpy change $\Delta H_{\text{encaps}}^{VH}$ are found, while the signs of the corresponding effective $\Delta S_{\text{encaps}}^{VH}$ are different. The methyl group of $\text{OC}(\text{O})\text{CH}_3$ at the end of the guest molecule is more strongly interacting with that of COOCH_3 .

For clear understanding of the guest-host interaction inside of the capsule, Haino and his coworkers extended the study by synthesizing the deuterium guest molecules having CD_3 at the ends of molecules. They performed the competition experiments



and succeeded in determining the ratio of the equilibrium constants $K_{\text{D}}^{eq}/K_{\text{H}}^{eq}$ and its temperature dependence⁶ by comparing the integrated signal intensity of the methyl protons versus the phenyl, the methyne or the methylene protons adjacent to the acetyl groups of the guest molecule inside of and outside of the host molecule. The Van't Hoff plot of the equilibrium constants $K_{\text{D}}^{eq}/K_{\text{H}}^{eq}$ yields the isotope change of the Gibbs free energy change $\Delta_{\text{D-H}}\Delta G_{\text{encaps}}$ as

Table 1.

Guest molecule	$\Delta H_{\text{H}}^{\text{VH}}$ /kJ/mol	$\Delta S_{\text{H}}^{\text{VH}}$ /J/mol/K	K_{H}^{eq}	$\Delta_{\text{D-H}}\Delta H^{\text{VH}}$ /kJ/mol	$\Delta_{\text{D-H}}\Delta S^{\text{VH}}$ /J/mol/K	$K_{\text{D}}^{\text{eq}}/K_{\text{H}}^{\text{eq}}$	T/K
A ₁ BBA ₁	-23.5 ± 0.3	+17.6 ± 0.8	8.2 × 10 ⁴ ± 2 × 10 ³	-1.96 ± 0.03	-5.4 ± 0.1	1.17	at 293
A ₂ BBA ₂	-6.49 ± 0.33	+28.5 ± 2.1	4.1 × 10 ² ± 1 × 10 ¹	-3.59 ± 0.07	-12.6 ± 0.3	1.19	at 263
A ₁ C ₄ C ₉ L ₁ A ₁	-32.7 ± 0.8	-10.0 ± 3.3	17 × 10 ⁴ ± 2 × 10 ⁴	-3.75 ± 0.09	-10.4 ± 0.3	1.35	at 293
A ₂ (CH ₂) ₄ A ₂	-10.0 ± 0.4	+24.7 ± 2.5	4.9 × 10 ² ± 5 × 10 ²	-2.61 ± 0.04	-8.1 ± 0.2	1.31	at 263

The guest molecules and their naming are given in Figure 2. The second and third columns are the slope $\Delta H_{\text{H}}^{\text{VH}}$ and the intercept $\Delta S_{\text{H}}^{\text{VH}}$ of Van't Hoff plots (2) for encapsulation equilibrium and the equilibrium constants in the fourth column for the guest molecules having all C¹H₃⁵⁹. The subscript H of H_{H}^{VH} , S_{H}^{VH} , and K_{H}^{eq} notifies it. The fifth and sixth columns are the isotope changes of the slopes $\Delta_{\text{D-H}}\Delta H^{\text{VH}}$ and the intercept $\Delta_{\text{D-H}}\Delta S^{\text{VH}}$ of Van't Hoff plots (4) for competition equilibrium evaluated for the ratio of the equilibrium constants $K_{\text{D}}^{\text{eq}}/K_{\text{H}}^{\text{eq}}$ ⁶⁰.

$$\ln(K_{\text{D}}^{\text{eq}}/K_{\text{H}}^{\text{eq}}) = -\frac{\Delta_{\text{D-H}}\Delta G_{\text{encaps}}}{RT} = -\frac{\Delta_{\text{D-H}}\Delta H_{\text{encaps}}^{\text{VH}}}{RT} + \Delta_{\text{D-H}}\Delta S_{\text{encaps}}^{\text{VH}} \quad (4)$$

The determined slope $\Delta_{\text{D-H}}\Delta H_{\text{encaps}}^{\text{VH}}$ and intercept $\Delta_{\text{D-H}}\Delta S_{\text{encaps}}^{\text{VH}}$ are shown in Table 1.

The characteristic findings on the isotope effects in Table 1 are summarized as

1. The substantial increase of the equilibrium constant is found by the deuteration.
2. The slopes $\Delta_{\text{D-H}}\Delta H_{\text{encaps}}^{\text{VH}}$ are negative for all four guest molecules. It apparently implies that the deuterated guest molecules more strongly bound to the capsule than the protiated guests.
3. The intercept $\Delta_{\text{D-H}}\Delta S_{\text{encaps}}^{\text{VH}}$ are also negative for all guest molecules. It implies that the encapsule equilibrium for the deuterated guest is entropically less favored than for the protiated guest.
4. Both $\Delta_{\text{D-H}}\Delta H_{\text{encaps}}^{\text{VH}}$ and $\Delta_{\text{D-H}}\Delta S_{\text{encaps}}^{\text{VH}}$ are not simply correlated to $\Delta H_{\text{H}}^{\text{VH}}$ and $\Delta S_{\text{H}}^{\text{VH}}$, respectively.

Among these findings, the large negative $\Delta_{\text{D-H}}\Delta S_{\text{encaps}}^{\text{VH}}$ is very suggestive to identify the cause of the observed isotope effects. The entropy change is related to the number of quantum levels involved in the process. For instance, even if the C-H bond length and its vibrational frequency are changed by the deuteration and by the encapsulation, the entropy is not changed at all. It is because at room temperature only the single zero-point vibration level is involved both in the protiated and deuterated molecules. The experimentally observed large change in $\Delta_{\text{D-H}}\Delta S_{\text{encaps}}^{\text{VH}}$ excludes the normal isotope effects in the molecules having the CH bonds.

If the above observed findings in the isotope effects could be even qualitatively explained with any model, the structure and dynamics of the self-assembled encapsulation can be elucidated. In the following sections, we attempt to evaluate the isotope effects on the Gibbs free energy $\Delta_{\text{D-H}}\Delta G_{\text{encaps}}$ with a simple model, and then to compare the corresponding quantities of the slope $\Delta_{\text{D-H}}\Delta H_{\text{encaps}}^{\text{VH}}$ and the intercept $\Delta_{\text{D-H}}\Delta S_{\text{encaps}}^{\text{VH}}$ of the Van't Hoff plots with the experimental data given in Table 1.

THEORETICAL MODEL

Thermochemical Functions of the encapsulating cluster and the change by the deuteration

Before examining the experimentally observed large isotope effects on the thermochemical functions, we first review the basics of the changes of the thermochemical functions in the encapsulation equilibrium (1). The partition functions of the components are approximately factorized as

$$Z_{\text{AG}}(\text{X}) = Z_{\text{AG}}^{\text{el}} Z_{\text{AG}}^{\text{vib-A}} Z_{\text{AG}}^{\text{vib-G}'} Z_{\text{AG}}^{\text{CX}}(\text{X}) Z_{\text{AG}}^{\text{inter-v}}(\text{X}) Z_{\text{AG}}^{\text{i-T}}(\text{X}) Z_{\text{AG}}^{\text{rot}} Z_{\text{AG}}^{\text{tr}} Z_{\text{AG}}^{\text{solv}} \quad (5)$$

$$Z_{\text{A}} = Z_{\text{A}}^{\text{el}} Z_{\text{A}}^{\text{vib-A}} Z_{\text{A}}^{\text{rot}} Z_{\text{A}}^{\text{tr}} Z_{\text{A}}^{\text{solv}} \quad (6)$$

$$Z_{\text{G}}(\text{X}) = Z_{\text{G}}^{\text{el}} Z_{\text{G}}^{\text{vib-G}'} Z_{\text{G}}^{\text{CX}}(\text{X}) Z_{\text{G}}(\text{X}) Z_{\text{G}}^{\text{rot}} Z_{\text{G}}^{\text{tr}} Z_{\text{G}}^{\text{solv}} \quad (7)$$

Here Z^{el} , Z^{vib} , Z^{rot} and Z^{tr} are the electronic, vibrational, rotational and translational parts of the partition functions for each component, respectively. The last factor Z^{solv} is the contribution from the solvent-solute

interaction. The contributions from the internal rotation (Z^{i-r}) and from the CX ($X=H$ or D) vibration (Z^{CX}) of the methyl groups are explicitly written in the equation, because our present concern is the change induced by the replacement of the light hydrogen $H(^1H)$ atoms of the methyl group with the heavy hydrogen $D(^2H)$. The contribution from the other intramolecular vibrations is $Z^{vib-G'}$. Because the mass of the host molecule A is much larger than that of the guest molecule, the intermolecular vibrations are considered to be the translational and torsional motions of the guest molecule inside of the capsule. As will be discussed later, the torsional motions of a whole guest molecule inside of the capsule is possibly coupled with the internal rotations of the end methyl groups, but for the time being, it is assumed that they are approximately separated.

The Gibbs free energy change in the encapsulation equilibrium (1) is

$$\Delta G_{encaps}(X) = -kT[\ln Z_{AG}(X) - \{\ln Z_A + \ln Z_G(X)\}] = -kT \ln \frac{Z_{AG}(X)}{Z_A Z_G(X)} \quad (8)$$

$$= -kT \left\{ \begin{aligned} & \ln \left(\frac{Z_{AG}^{el}}{Z_A Z_G^{el}} \right) + \ln \left(\frac{Z_{AG}^{rot}}{Z_A Z_G^{rot}} \right) + \ln \left(\frac{Z_{AG}^{tr}}{Z_A Z_G^{tr}} \right) + \ln \left(\frac{Z_{AG}^{solv}}{Z_A Z_G^{solv}} \right) + \ln \left(\frac{Z_{AG}^{vib-A}}{Z_A Z_G^{vib-A}} \right) \\ & + \ln \left(\frac{Z_{AG}^{vib-G'}}{Z_G^{vib-G'}} \right) + \ln \left(\frac{Z_{AG}^{CX}(X)}{Z_G^{CX}(X)} \right) + \ln \left(\frac{Z_{AG}^{i-r}(X)}{Z_G^{i-r}(X)} \right) + \ln Z_{AG}^{inter-v}(X) \end{aligned} \right\} \quad (9)$$

by assuming that the partial derivative of the partition function on "volume" is neglected. The main term in the free energy change in the chemical equilibrium is the first term resulting from the difference of the total electronic energies before and after the encapsulation, which is governed by the non-covalent molecular interaction between the host and guest molecules. Importantly in the present case, the electronic energy is not changed by the deuteration of the methyl group. The change by the deuteration of the Gibbs free energy change is

$$\Delta_{D-H} \Delta G_{encaps} = \Delta G_{encaps}(D) - \Delta G_{encaps}(H) \quad (10)$$

Hereafter, the subscript *encaps* is removed for simplicity. Because the mass, volume, and inertia moments of the guest molecule are not changed much by the deuteration of the methyl groups, the terms in the first six terms of equation (9) are expected not to contribute to the difference $\Delta_{D-H} \Delta G$. Thus, the change of the Gibbs free energy change (the double delta, we may call it) by the deuteration is

$$\Delta_{D-H} \Delta G \simeq -kT \left[\ln \left(\frac{Z_{AG}^{CX}(D)}{Z_G^{CX}(D)} \right) - \ln \left(\frac{Z_{AG}^{CX}(H)}{Z_G^{CX}(H)} \right) \right] - kT \left[\ln \left(\frac{Z_{AG}^{i-r}(D)}{Z_G^{i-r}(D)} \right) - \ln \left(\frac{Z_{AG}^{i-r}(H)}{Z_G^{i-r}(H)} \right) \right] \quad (11)$$

$$\begin{aligned} & -kT \left[\ln Z_{AG}^{inter-v}(D) - \ln Z_{AG}^{inter-v}(H) \right] \\ & = -kT \left[\ln \left(\frac{Z_{AG}^{CX}(D)}{Z_{AG}^{CX}(H)} \right) - \ln \left(\frac{Z_G^{CX}(D)}{Z_G^{CX}(H)} \right) \right] - kT \left[\ln \left(\frac{Z_{AG}^{i-r}(D)}{Z_{AG}^{i-r}(H)} \right) - \ln \left(\frac{Z_G^{i-r}(D)}{Z_G^{i-r}(H)} \right) \right] \\ & -kT \ln \left(\frac{Z_{AG}^{inter-v}(D)}{Z_{AG}^{inter-v}(H)} \right) \end{aligned} \quad (12)$$

Here in (12), the augments of \ln are rearranged to make the isotope effects clear. Similarly the double delta $\Delta_{D-H} \Delta H$ for the enthalpy change is written by the partition functions as

$$\begin{aligned} \Delta_{D-H} \Delta H & \simeq -\frac{\partial}{\partial \beta} \left[\ln \left(\frac{Z_{AG}^{CX}(D)}{Z_{AG}^{CX}(H)} \right) - \ln \left(\frac{Z_G^{CX}(D)}{Z_G^{CX}(H)} \right) \right] \\ & -\frac{\partial}{\partial \beta} \left[\ln \left(\frac{Z_{AG}^{i-r}(D)}{Z_{AG}^{i-r}(H)} \right) - \ln \left(\frac{Z_G^{i-r}(D)}{Z_G^{i-r}(H)} \right) \right] -\frac{\partial}{\partial \beta} \left[\ln \left(\frac{Z_{AG}^{inter-v}(D)}{Z_{AG}^{inter-v}(H)} \right) \right] \end{aligned} \quad (13)$$

We first examine the contribution of the CH stretching motions from the first term in (12) and (13), which is the most well-known deuteration effect among the chemists⁹⁾. Because the C-X ($X=H$ and D) stretching modes are nearly harmonic and the frequency shift by the encapsulation can be approximately evaluated, the contribution of the C-X modes to $\Delta_{D-H} \Delta H$ can be estimated as

$$\begin{aligned}
& -\frac{\partial}{\partial\beta} \left[\ln \left(\frac{Z_{AG}^{CX}(D)}{Z_{AG}^{CX}(H)} \right) - \ln \left(\frac{Z_G^{CX}(D)}{Z_G^{CX}(H)} \right) \right] \\
& \simeq 2*3*\frac{\hbar}{2} [(\nu_{AG}^D - \nu_{AG}^H) - (\nu_G^D - \nu_G^H)] \\
& \simeq 3\hbar \left(\frac{1}{\sqrt{2}} - 1 \right) (\nu_{AG}^H - \nu_G^H)
\end{aligned} \tag{14}$$

where only the zero point vibration is assumed to contribute to the sum in the partition function, and $\nu^D \simeq \frac{1}{\sqrt{2}}\nu^H$ is also assumed. The factor 2 in the second line is for two methyl groups of the guest molecule and the factor 3 is for three C-X bonds of the methyl group. In the capsule, the methyl groups of the guest molecule are interacted with the aromatic rings of the host molecule, and the shift $(\nu_{AG}^H - \nu_G^H)$ is negative and about -10 cm^{-1} ⁸⁾. Contrary to the experimental findings, the term (14) becomes positive and about $+1 \text{ kJ/mol}$. More importantly, the change of the CH frequency and also the change of the bond length by the encapsulation and by the isotope replacement cannot account for the double change of the entropy, $\Delta_{D-H}\Delta S$, because at the experimental temperature, only the zero point level of the CH vibrations is populated. So we can safely exclude the CH frequency change by the encapsulation as a possible candidate for the observed deuteration effects.

The second term in (12) and (13) is the contribution of the internal rotation of the methyl group relative to the main frame of the guest molecules. The quantum level spacings of the methyl rotation are sensitive to the mass of the hydrogen atom, and also to the barrier height V_h of the rotation. Inside of the capsule the methyl groups at both ends of the guest molecule are interacted with the host molecule, most possibly at the aromatic rings of the host molecule. This interaction does change the barrier height of the methyl rotation. Thus, the contribution of the methyl internal rotation is the best candidate to the double delta $\Delta_{D-H}\Delta G$ in the thermochemical functions.

The third term in (12) and (13) is the one from the intermolecular vibrations. There are six modes; three are from the translational motions and the other three from the rotational motion of the guest molecule inside of the capsule. Because of their low frequency motions, the contribution to the thermochemical functions such as ΔG_{encaps} is expected to be very much temperature-dependent, and thus if the chemical equilibrium (1) itself is concerned with, this term might play an important role in the temperature dependent terms. The question is whether these intermolecular motions influence the deuteration effects. The mass ratio and also the effective volume ratio of the methyl groups to the whole guest molecule is small. For instance, the mass of the smallest guest molecule $A_2(CH_2)_8A_2$ changes from 214 to 220 by the deuteration of the methyl groups. Among the six intermolecular motions, one of the torsional motions, whose axis is approximately parallel to the internal rotation axis of the methyl group, might be coupled with the methyl rotations, and the quantum levels possibly are influenced by the deuteration. The inertia moments around the axes perpendicular to the long molecular axis are expected to be changed by the deuteration of the methyl groups, because they are located far away from the center of masses.

In the following subsections, the contribution from the methyl internal rotation is theoretically and numerically examined.

Schrödinger equation of the internal rotation

In the classical textbook of "Thermodynamics" by Pitzer and Brewer¹⁰⁾, the thermochemical functions for the periodical potential energy functions, which include the potential energy function for a methyl internal rotation, are tabulated in the book. It is because the energy spectrum of those periodic potentials can be obtained only numerically. Those tables are the products of Pitzer himself and his coworkers¹¹⁾¹²⁾¹³⁾.

The Schrödinger equation for the internal rotation was solved soon after Quantum mechanics was established¹⁴⁾. The Schrödinger equation with a periodic potential function such as

$$H(\theta)\Phi_K(\theta) = \left[-\frac{\hbar^2}{2I_e} \frac{\partial^2}{\partial \theta^2} + \frac{V_h}{2}(1 - \cos \kappa\theta) \right] \Phi_K(\theta) = \varepsilon_K \Phi_K(\theta) \quad (15)$$

can be solved by expanding the wave function in terms of $\cos(m\kappa\theta)$ and $\sin(m\kappa\theta)$. The equation is transformed to the infinite tri-diagonal hamiltonian matrix equation. By dividing equation¹⁵⁾ by $\left(\frac{\hbar^2}{I_e}\right)$, the hamiltonian becomes dimensionless with a single parameter η

$$\eta \equiv \frac{V_h}{\left(\frac{\hbar^2}{I_e}\right)} = \frac{I_e V_h}{\hbar^2} \quad (16)$$

as

$$\hat{h}(\theta; \eta)\Phi_K(\theta; \eta) = \left[-\frac{1}{2} \frac{\partial^2}{\partial \theta^2} + \frac{\eta}{2}(1 - \cos \kappa\theta) \right] \Phi_K(\theta; \eta) \quad (17)$$

$$= \varepsilon_K(\eta)\Phi_K(\theta; \eta) \quad (18)$$

For the methyl rotation, $\kappa=3$, and the wave functions of even symmetry are

$$\Phi_{Kg}(\theta; \eta) = \sum_{m=0} a_{mK}(\eta) \cos(3m\theta) \quad (19)$$

and those of odd symmetry are

$$\Phi_{Ku}(\theta; \eta) = \sum_{m=1} b_{mK}(\eta) \sin(3m\theta) \quad (20)$$

Note that for the even functions the sum starts at $m=0$. By inserting equation (19) into equation (17) and multiply $\cos(3n\theta)$ on both sides of the equation, the integration over θ yields the matrix eigenvalue problem

$$\begin{bmatrix} \eta/2 & -\eta/4 & 0 & 0 & 0 & 0 & 0 \\ -\eta/4 & (9+\eta)/2 & -\eta/4 & 0 & 0 & 0 & 0 \\ 0 & -\eta/4 & (9*2^2+\eta)/2 & -\eta/4 & 0 & 0 & 0 \\ 0 & 0 & -\eta/4 & (9*3^2+\eta)/2 & -\eta/4 & 0 & 0 \\ \vdots & \dots & \dots & \dots & \ddots & \vdots & \vdots \\ \vdots & \dots & \dots & \dots & \dots & \ddots & \vdots \\ \vdots & \dots & \dots & \dots & \dots & \dots & \ddots \end{bmatrix} \begin{bmatrix} a_0 \\ a_1 \\ a_2 \\ a_3 \\ a_4 \\ \vdots \\ \vdots \\ \vdots \end{bmatrix} = \varepsilon_K \begin{bmatrix} a_0 \\ a_1 \\ a_2 \\ a_3 \\ a_4 \\ \vdots \\ \vdots \\ \vdots \end{bmatrix} \quad (21)$$

which can be numerically solved quickly by a subroutine for the tri-diagonal matrix eigenvalue problem in LAPACK, even for the dimension=200. The equation for the odd symmetry is

$$\begin{bmatrix} (9+\eta)/2 & -\eta/4 & 0 & 0 & 0 & 0 \\ -\eta/4 & (9*2^2+\eta)/2 & -\eta/4 & 0 & 0 & 0 \\ 0 & -\eta/4 & (9*3^2+\eta)/2 & -\eta/4 & 0 & 0 \\ \vdots & \dots & \dots & \ddots & \vdots & \vdots \\ \vdots & \dots & \dots & \dots & \ddots & \vdots \\ \vdots & \dots & \dots & \dots & \dots & \ddots \end{bmatrix} \begin{bmatrix} b_1 \\ b_2 \\ b_3 \\ b_4 \\ \vdots \\ \vdots \\ \vdots \end{bmatrix} = \varepsilon_K \begin{bmatrix} b_1 \\ b_2 \\ b_3 \\ b_4 \\ \vdots \\ \vdots \\ \vdots \end{bmatrix} \quad (22)$$

Although their eigenvalues are expanded by the continued fractions as

$$\varepsilon_K = \frac{\eta}{2} - \frac{\left(\frac{\eta}{4}\right)}{2\left\{\frac{9*1^2}{\eta} + 1 - \frac{2\varepsilon_K}{\eta}\right\}} - \frac{\left(\frac{\eta}{4}\right)}{2\left\{\frac{9*2^2}{\eta} + 1 - \frac{2\varepsilon_K}{\eta}\right\}} - \dots$$

for even states and

$$\varepsilon_K = \left(9 + \frac{\eta}{2}\right) - \frac{\left(\frac{\eta}{4}\right)}{2\left\{\frac{9*2^2}{\eta} + 1 - \frac{2\varepsilon_K}{\eta}\right\}} - \frac{\left(\frac{\eta}{4}\right)}{2\left\{\frac{9*3^2}{\eta} + 1 - \frac{2\varepsilon_K}{\eta}\right\}} - \dots$$

for odd states, but they are numerically useless.

Internal rotational states of a methyl group

The inertia moment of a methyl around the C_3 axis is

$$I_{CX_3}/M_X = \sum_{i=1}^3 (x_i^2 + y_i^2) \quad (23)$$

$$= \frac{24}{9}R^2 \quad (24)$$

if the tetrahedral configuration is assumed. Because the methyl group is connected with the molecular unit of a finite principal inertia moment I_A , the effective inertia moment is

$$\frac{1}{I_{effX}} = \frac{1}{I_{CX_3}} + \frac{1}{I_G} \quad \text{or} \quad (25)$$

$$I_{effX} \simeq I_{CX_3} \left(1 - \frac{I_{CX_3}}{I_G}\right) \quad (26)$$

This equation assumes that the rotation axes of CX_3 and unit G are parallel to each other. If the axes are skewed, the effective inertia moment is

$$I_{effX} \simeq I_{CX_3} \left(1 - I_{CX_3} \sum_{k=1}^3 \frac{\lambda_k^2}{I_{Gk}}\right) \quad (27)$$

where I_{Gk} is the k th component of the principal inertia moment and λ_k is the directional cosine between the k th principal axis of G and the C_3 axis of methyl group. In the following calculations, $I_{effX} = I_{CX_3}$ is assumed; the coupling with the torsional motion of the main part of molecule G is not explicitly taken into account.

As given in (16), the parameter η in the dimensionless hamiltonian is $\frac{I_{effX}V_h}{\hbar^2}$, and therefore the calculated results using $I = I_{CX_3}$ for a barrier V_h corresponds to the barrier

$$V_{h_real} = \left(1 - I_{CX_3} \sum_{k=1}^3 \frac{\lambda_k^2}{I_{Gk}}\right) V_h \quad (28)$$

if the coupling with the rotation of the main frame is taken into account through the inertia moment.

As is given in equation (16), the energy unit of the dimensionless hamiltonian is $\left(\frac{\hbar^2}{I_{eff}}\right)$, which is 0.126382 kJ/mol for CH_3 and 0.063222 kJ/mol for CD_3 . It implies that the energy parameter η in the dimensionless hamiltonian is much larger than 1 even for the low energy barrier such as $V_h = 3$ kJ/mol.

Figure 3 shows the energy levels for $V_h = 5, 9$ and 39 kJ/mol together with the potential energy curve. Near and over the barrier, the even and odd states are nearly degenerated, and it is clear that the quantum levels for CD_3 (the red lines of the right side) are more dense than for CH_3 (the blue lines of the left side).

Figure 4 shows how the energy levels of the internal rotations of CH_3 and CD_3 change with the barrier height V_h . Both figures show that the number of the states relevant to the thermochemical properties at the experimental temperature ($RT_{300K} = 2.52$ and $RT_{263K} = 2.186$ kJ/mol) is not large, but for a low barrier, a few states contribute to the partition function. For a high barrier, from at least two lowest states (0 e and 1 o labeled in the figures) is expected to be important. For a large integer K , the energy is approximately written as

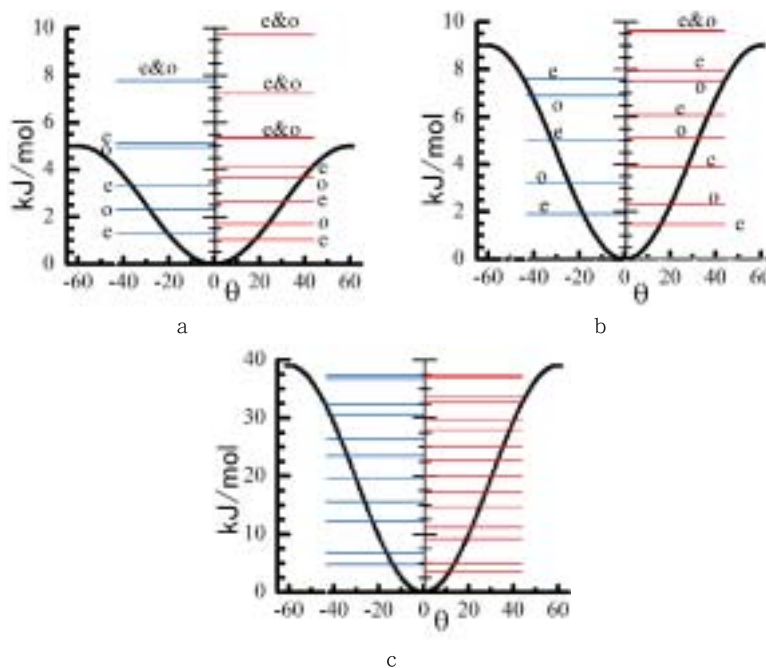


Figure 3. The potential energy curves and the internal rotation levels. The marks e and o stand for the state of the symmetry.
a) for $V_h = 5$ kJ/mol, b) for $V_h = 9$ kJ/mol, c) for $V_h = 39$ kJ/mol.

$$\varepsilon_K \simeq \frac{1}{2} \left[(3K)^2 \frac{\hbar^2}{I_{eff}} + V_h \right] \text{ kJ/mol for both odd and even states} \quad (29)$$

and Figure 4 demonstrates that this approximation does hold well for $K \geq 4$ and $V_h < 25$ in CH_3 and for $K \geq 6$ and $V_h < 25$ for CD_3 . But the energies for the lower levels cannot simply be expressed analytically. It turns out that the energy of the low-lying states can be expanded in terms of the polynomial of the dimensionless parameter $(\eta)^{1/2}$. The fourth order plots for states e0 and o1, the lowest state of each symmetry, are accurate; the root square mean error is 0.999998 up to $\eta=500$. The second order plots also reasonably accurate; the root square mean error is 0.9998. The second order expression for these two states is

$$\varepsilon_K(X, V) = c_K^{(0)} \frac{\hbar^2}{I_X} + c_K^{(1)} V_h^{1/2} \left(\frac{\hbar^2}{I_X} \right)^{1/2} + c_K^{(2)} V \quad (30)$$

with $(c_{e0}^{(0)}, c_{e0}^{(1)}, c_{e0}^{(2)}) = (0, 1.6736658, 0.0253763)$ and
with $(c_{o1}^{(0)}, c_{o1}^{(1)}, c_{o1}^{(2)}) = (9/2, 2.4311447, 0.0213837)$

The second term is a product of $V_h^{1/2}$ and $\left(\frac{\hbar^2}{I_X} \right)^{1/2}$; this term represents the coupling with the potential energy barrier and the inertia moment and plays a key role in the double delta.

The higher energy levels approximated in equation (29) contribute to the double delta $\Delta_{D-H}\Delta$ by the encapsulation only through the change of the population; the change of the energy levels induced by the increase of the barrier height V_h is independent of the inertia moment. So the lower energy levels, whose energies cannot be approximated by (29), are important in examining the contribution from the internal rotation to the isotope effects on the encapsulation equilibrium. In the following we first examine the isotope effects numerically by taking into account all of the quantum levels, and then to demonstrate how the second term of equation (30) influences the double delta $\Delta_{D-H}\Delta$, the two-state model is briefly discussed.

Nuclear spin statistical weight

To evaluate the partition function of the methyl rotation, the nuclear spin statistical weight for the quantum levels has to be considered. The internal rotational wave functions $\Phi_{ir}(\theta)$ of the methyl rotation of

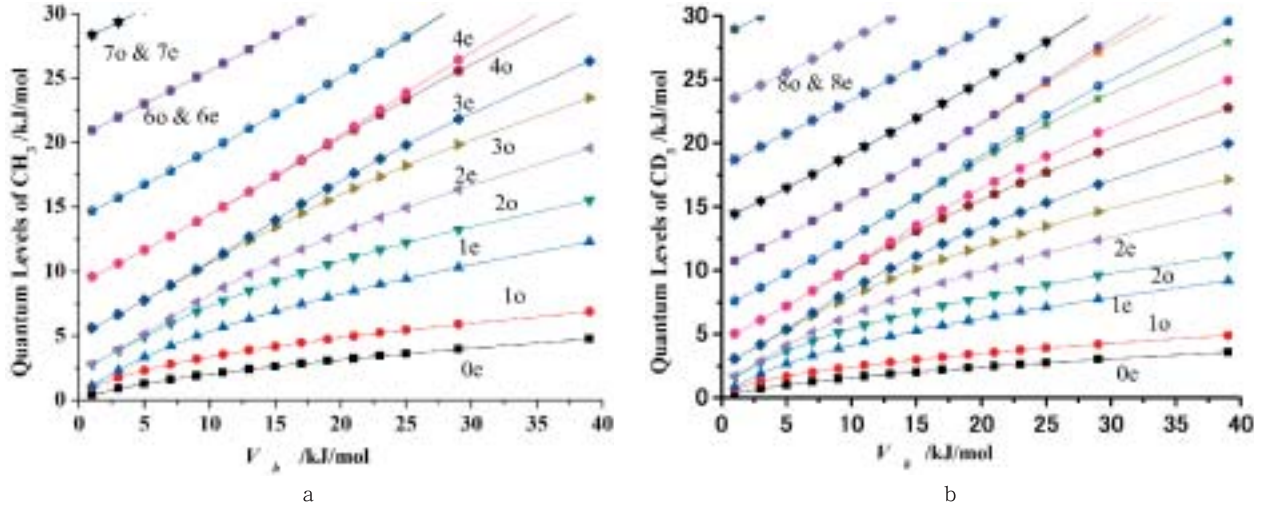


Figure 4. The V_h dependence of the internal rotational quantum levels.
a) For CH_3 , b) For CD_3 .

molecule XCH_3 are classified by the sign change of the wave function when the angle θ is changed to $-\theta$. The total wave function $\Psi(\theta, I_1, I_2, I_3)$ of the methyl rotation including the nuclear spin wave function $\Phi_{ns}(I_1, I_2, I_3)$ should satisfy the nuclear spin statics. For instance, operate the mirror operation $\hat{\sigma}_1$ onto $\Psi(\theta, I_1, I_2, I_3)$, by assuming that the plane passes the hydrogen atom 1 and the carbon, and that the angle θ is measured from that plane,

$$\begin{aligned} \hat{\sigma}_1 \Psi(\theta, I_1, I_2, I_3) &= \hat{\sigma}_1 \{ \Phi_{ir}^{\Gamma}(\theta) \Phi_{ns}^{\Gamma}(I_1, I_2, I_3) \} \\ &= \{ \hat{\sigma}_1 \Phi_{ir}^{\Gamma}(\theta) \} \{ \hat{\sigma}_1 \Phi_{ns}^{\Gamma}(I_1, I_2, I_3) \} \\ &= \Phi_{ir}^{\Gamma}(-\theta) \Phi_{ns}^{\Gamma}(I_1, I_2, I_3) \\ &= \{ \Gamma_{ir} \Phi_{ir}^{\Gamma}(\theta) \} \{ \Gamma_{ns} \Phi_{ns}^{\Gamma}(I_1, I_2, I_3) \} \\ &= \Gamma_{ir} \Gamma_{ns} \Psi(\theta, I_1, I_2, I_3) \end{aligned}$$

where we assume

$$\begin{aligned} \Phi_{ir}^{\Gamma}(-\theta) &= \Gamma_{ir} \Phi_{ir}^{\Gamma}(\theta), \\ \Gamma_{ir} &= +1 \text{ for even functions} \\ &= -1 \text{ for odd functions} \end{aligned}$$

and

$$\Phi_{ns}^{\Gamma}(I_1, I_2, I_3) = \Gamma_{ns} \Phi_{ns}^{\Gamma}(I_1, I_2, I_3)$$

where Γ_{ns} is the eigenvalue of the interchange operator $\hat{P}(2,3)$ as

$$\hat{P}(2,3) \Phi_{ns}^{\Gamma}(I_1, I_2, I_3) = \Phi_{ns}^{\Gamma}(I_1, I_3, I_2) = \Gamma_{ns} \Phi_{ns}^{\Gamma}(I_1, I_2, I_3)$$

The product $\Gamma_{ir} \Gamma_{ns}$ has to be a characteristic value for the nuclear species depending on the boson or fermion as

$$\begin{aligned} \Gamma_{ir} \Gamma_{ns} &= -1 \text{ for } \text{CH}_3 \\ &= +1 \text{ for } \text{CD}_3 \end{aligned}$$

Thus, for CH_3

$$\begin{aligned} \Gamma_{ns} &= -1 \text{ for even functions} \\ &= +1 \text{ for odd functions} \end{aligned}$$

for CD_3

$$\begin{aligned} \Gamma_{ns} &= +1 \text{ for even functions} \\ &= -1 \text{ for odd functions.} \end{aligned}$$

The eigenvalue of the interchange operator for the spin eigen functions $\Phi_{ns}(I, M_I; k)$ is determined by the total spin I of the function. For instance, the nuclear spin wave functions for H_2 are, as well known for the para and ortho hydrogen molecule,

$$\begin{aligned}\Phi_{ns}(1, +1; 1) &= \alpha(1)\alpha(2) & \Gamma_{ns} &= +1 \\ \Phi_{ns}(0, 0; 1) &= \frac{1}{\sqrt{2}}(\alpha(1)\beta(2) + \beta(1)\alpha(2)) & \Gamma_{ns} &= +1 \\ \Phi_{ns}(1, -1; 1) &= \beta(1)\beta(2) & \Gamma_{ns} &= +1 \\ \Phi_{ns}(0, 0; 1) &= \frac{1}{\sqrt{2}}(\alpha(1)\beta(2) - \beta(1)\alpha(2)) & \Gamma_{ns} &= -1\end{aligned}$$

Similarly the nuclear spin eigen functions of the H_3 part of CH_3 are $\Phi_{ns}(3/2, M_I; 1)$, $\Phi_{ns}(1/2, M_I; 1)$, and $\Phi_{ns}(1/2, M_I; 2)$ with $M_I = +I, +(I-1), \dots, -(I-1), -I$. The explicit forms of $\Phi_{ns}(3/2, +3/2; 1)$ and $\Phi_{ns}(3/2, -3/2; 1)$ are

$$\begin{aligned}\Phi_{ns}(3/2, +3/2; 1) &= \alpha(1)\alpha(2)\alpha(3) \\ \Phi_{ns}(3/2, -3/2; 1) &= \beta(1)\beta(2)\beta(3)\end{aligned}$$

which implies that $\Gamma_{ns} = +1$ for the wave function for $I=3/2$. The wave functions for $\Phi_{ns}(1/2, +1/2; k)$ for $k=1, 2$ are proper linear combinations of $\alpha(1)\alpha(2)\beta(3)$, $\alpha(1)\beta(2)\alpha(3)$ and $\beta(1)\alpha(2)\alpha(3)$ with $\Gamma_{ns} = -1$. Thus, the number of possible nuclear spin functions for even functions is $(2 \times 3/2 + 1) = 4$ and that for odd functions is $2 \times (2 \times 1/2 + 1) = 4$; these values are called the spin statistical weights, w_s . The sum should be equal to 2^3 .

The nuclear spin eigen functions for the D_3 part of CD_3 are $\Phi_{ns}(3, M_I; 1)$, $\Phi_{ns}(2, M_I; 1)$, $\Phi_{ns}(2, M_I; 2)$, $\Phi_{ns}(1, M_I; 1)$, $\Phi_{ns}(1, M_I; 2)$, $\Phi_{ns}(1, M_I; 3)$, and $\Phi_{ns}(0, M_I; 1)$. The explicit forms of $\Phi_{ns}(3, 3; 1)$ and $\Phi_{ns}(3, -3; 1)$ are

$$\begin{aligned}\Phi_{ns}(3, +3; 1) &= |1, +1; 1 \rangle |1, +1; 2 \rangle |1, +1; 3 \rangle \\ \Phi_{ns}(3, -3; 1) &= |1, -1; 1 \rangle |1, -1; 2 \rangle |1, -1; 3 \rangle\end{aligned}$$

where $|1, m_s; j \rangle$ is the nuclear spin function of deuterium atom j . Thus, the eigen value Γ_{ns} of $\Phi_{ns}(3, M_I; 1)$ is $+1$. The eigen value Γ_{ns} of $\Phi_{ns}(I, M_I; k)$ is proved to be $(-1)^{[I]+1}$. The spin statistical weight for even functions is $(2 \times 3 + 1) + 3 \times (2 \times 1 + 1) = 16$, and the spin statistical weight for odd functions is $2 \times (2 \times 2 + 1) + (2 \times 0 + 1) = 11$; the sum is 3^3 . In evaluating the partition functions, these statistical weights have to be used.

Partition function of the methyl rotation and the auxiliary functions

The partition function of the internal rotation of a methyl group is a function of the barrier height V_h and temperature T as well as the mass of the hydrogen atom and is written as

$$Z^{i,r}(X, V_h; T) = \frac{1}{\sigma_s} \left[\sum_{K=0}^{\infty} w_{se}(X) \exp(-\beta \varepsilon_{Kg}(X, V_h)) + \sum_{K=1}^{\infty} w_{so}(X) \exp(-\beta \varepsilon_{Ku}(X, V_h)) \right] \quad (31)$$

where σ_s is a symmetry number and $\beta = \frac{1}{k_B T}$. The statistical weights $w_{se}(X)$ and $w_{so}(X)$ are determined in the previous subsection for $X=H$ and D . The weights are normalized to 1. The sum is taken till the term becomes smaller than a threshold value. Here it is assumed that the internal rotations of two methyl groups of both ends of a guest molecule is not coupled with each other. Because we are interested only in the deuteration effects, it is convenient to define an auxiliary function

$$\Xi_{D-H}(V_h; T) \equiv \ln \left(\frac{Z^{i,r}(D, V_h; T)}{Z^{i,r}(H, V_h; T)} \right) \quad (32)$$

By comparing this definition with equation (12), $\Delta_{D-H} \Delta G$ is now

$$\Delta_{D-H} \Delta G = -\beta^{-1} \{ \Xi_{D-H}(V_h^{AG}; T) - \Xi_{D-H}(V_h^G; T) \} \quad (33)$$

where V_h^{AG} is the barrier height of the methyl group in the encapsulated guest molecule and V_h^G is the barrier height if the guest molecule is outside of the capsule. In the computation, a new auxiliary function

$$\mathcal{Q}(V_h; T) \equiv -\beta^{-1} \Xi_{D-H}(V_h; T) \quad (34)$$

is defined, where $\beta \equiv k_B T$. At each temperature T it is this function that is evaluated for a given V_h . The change $\Delta_{D-H}\Delta G$ is

$$\Delta_{D-H}\Delta G = Q(V_h^{AG}; T) - Q(V_h^G; T) \quad (35)$$

which clearly indicates the “double” delta. Similarly the auxiliary function $\mathcal{H}(V_h; T)$ and $S(V_h; T)$ can be defined as

$$\mathcal{H}(V_h; T) \equiv -\frac{\partial}{\partial \beta} \Xi_{D-H}(V_h; T) \quad (36)$$

$$S(V_h; T) \equiv k_B \Xi_{D-H}(V_h; T) - \frac{1}{T} \frac{\partial}{\partial \beta} \Xi_{D-H}(V_h; T) \quad (37)$$

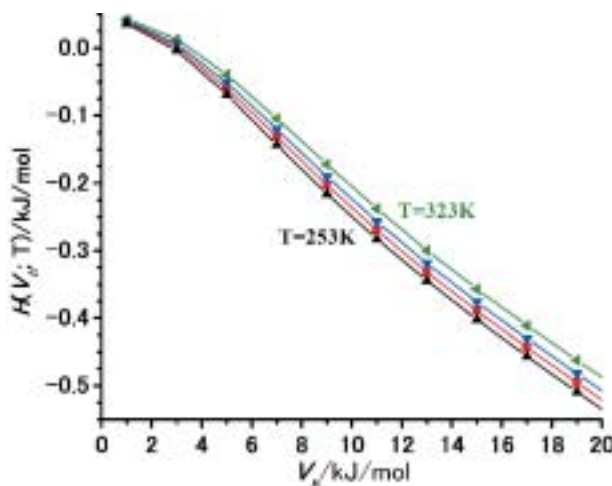


Figure 5. The auxiliary function $\mathcal{H}(V_h; T)$ for $T=323$ (leftward triangle), 293 (square), 273 (downward triangle) and 253 K (upward triangle).

Figure 5 shows the V_h dependence of the auxiliary function $\mathcal{H}(V_h; T)$, which is a decreasing function of the barrier height V_h . It implies that if the barrier height V_h increases by the encapsulation, the enthalpy change $\Delta_{D-H}\Delta H$ is negative, which is consistent with the experimental finding (2). Similarly, The auxiliary function $S(V_h; T)$ is also a decreasing function of V_h , again consistent with the finding (3). The cause of the negative values is discussed later.

COMPARISON WITH THE EXPERIMENTS

As Figure 5 shows, the function $\mathcal{H}(V_h; T)$ is temperature-dependent. The thermal energies at 323 K and 253 K are 2.93 kJ/mol and 2.10 kJ/mol, respectively, and thus, as is seen in Figures 3 and 4, the population of the lower levels is temperature-dependent at these temperatures. Therefore, the direct evaluation of $\Delta_{D-H}\Delta H$ in Figure 5 does not correspond to the slope of the Van't Hoff plots, which assumes that ΔH and ΔS are constant. In Figure 6, the “theoretical” Van't Hoff plots, $-\frac{\Delta_{D-H}\Delta G}{RT}$, are shown by assuming that the barrier height of the methyl internal rotation outside of the capsule is $V_h^G = 3\text{kJ/mol}$ in Figure 6a and $V_h^G = 9\text{kJ/mol}$ in Figure 6b. The slope and the intercept of these linear plots correspond to $\Delta_{D-H}\Delta H^{VH}$ and $\Delta_{D-H}\Delta S^{VH}$ in Table 1, respectively, and they are summarized as a function of the increase in the barrier height $\Delta V_h \equiv V_h^{GA} - V_h^G$ in Figure 7a and 7b. To draw the curves of Figure 7, the slope and the intercept of the plots in Figure 6 are multiplied by 2, by assuming that the methyl group of both ends of the guest molecule independently and equally contributes to the change of the thermochemical properties.

As is clearly shown in Figure 7, the estimated $\Delta_{D-H}^{\text{mod}el}\Delta H^{VH}$ is comparable to those $\Delta_{D-H}\Delta H^{VH}$ Table 1 determined by the experiments, though a rather large (30 to 90 kJ/mol) change $\Delta V_h \equiv V_h^{AG} - V_h^G$ in the

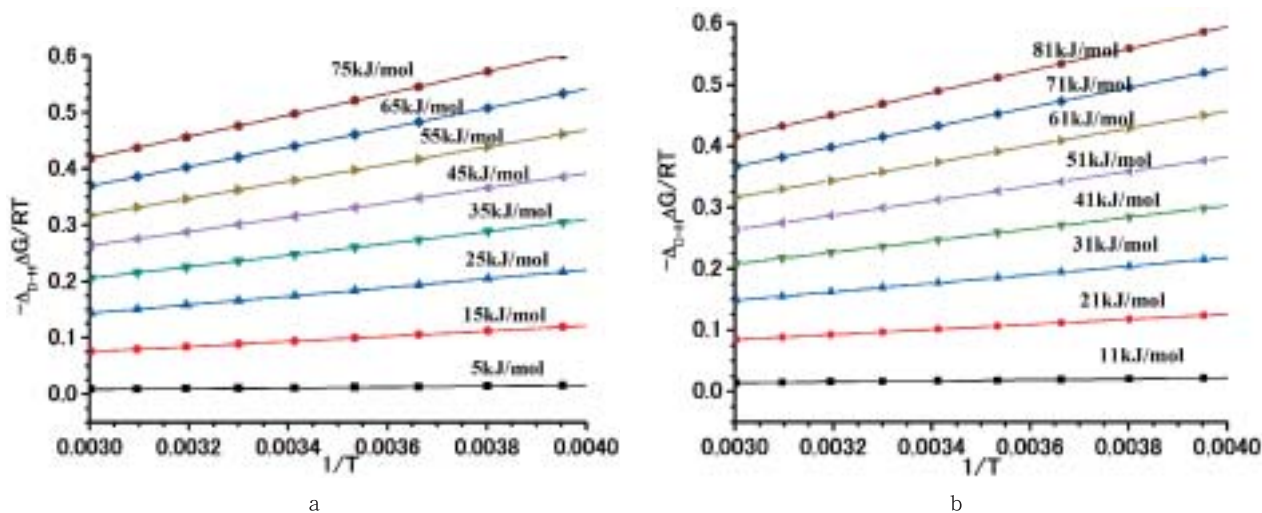


Figure 6. The “theoretical” Van't Hoff plots for several V_h^{AG} . In a) the barrier height $V_h^G = 3$ kJ/mol and in b) $V_h^G = 9$ kJ/mol is assumed.

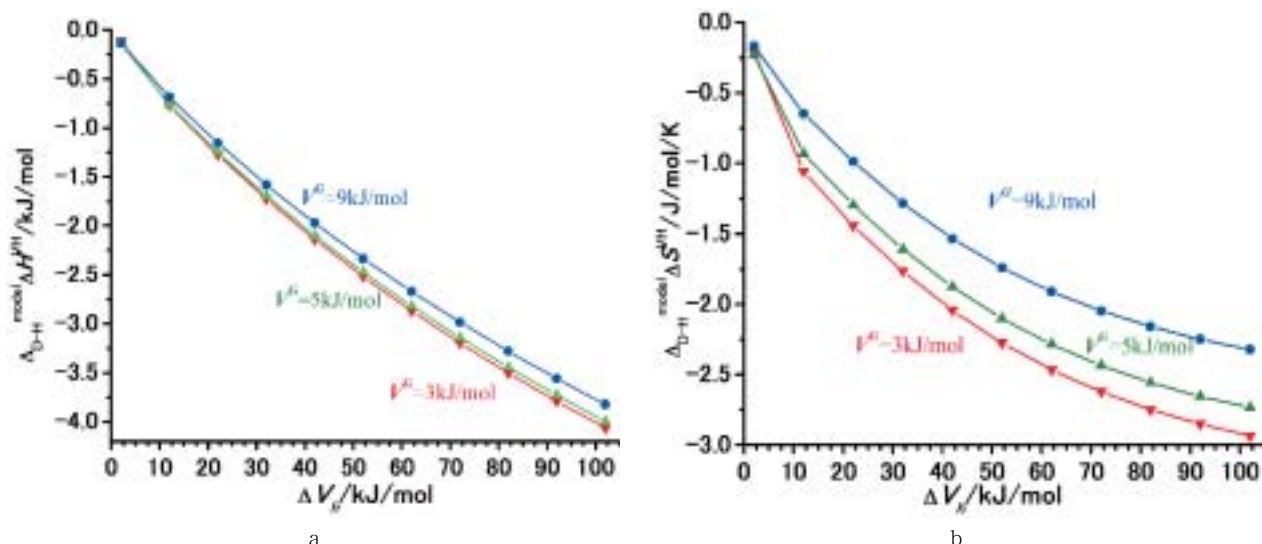


Figure 7. The theoretical double delta as a function of $\Delta V_h = V_h^{AG} - V_h^G$, a) $\Delta_{D-H}\Delta H^{mod el}$ and b) $\Delta_{D-H}\Delta S^{mod el}$ evaluated from the slope and intercept of the plots in Figure 6.

barrier height by the encapsulation has to be assumed. With the same change ΔV_h , however, the estimated $\Delta_{D-H}^{mod el}\Delta S^{mod el}$ is a half to a quarter of those numbers $\Delta_{D-H}\Delta S^{mod el}$ in Table 1.

The barrier height V_h^G of the methyl group of the guest molecule in solution is expected to be not high; less than 10 kJ/mol. The barrier height V_h^G for A_1BBA_1 with a preliminary MM2 calculation is 5 kJ/mol. Figure 7a indicates that $\Delta_{D-H}^{mod el}\Delta H^{mod el}$ is not sensible to V_h^G , but that $\Delta_{D-H}^{mod el}\Delta S^{mod el}$ is dependent on V_h^G ; the smaller V_h^G , the larger $|\Delta_{D-H}^{mod el}\Delta S^{mod el}|$. The ratio of the equilibrium constants $\left(\frac{K_D^{eq}}{K_H^{eq}}\right)$ can be evaluated using $-\frac{\Delta_{D-H}\Delta G}{RT}$.

As the experimental summary (1), the ratio is larger 1; because of the underestimation of $|\Delta_{D-H}^{mod el}\Delta S^{mod el}|$, the estimated ratios are too large for $V_h^G \approx 3$ to 9 kJ/mol and $\Delta V_h \approx 30$ to 90 kJ/mol.

Two-state model

Upto here, the figures are drawn based on the numerical calculations. To demonstrate which terms are the key in the negative signs in $\Delta_{D-H}^{mod el}\Delta H^{mod el}$, the enthalpy change is evaluated using the two-state model. Only the lowest state of each symmetry, e0 and o1, is taken into account. As is seen in Figure 4, the two-state model does work only for a high barrier. Their energies are approximated in equation (30). In evaluating the partition function, the high temperature approximation

$$\begin{aligned} \exp\{-\beta(\varepsilon_{o1}(\text{D}, V) - \varepsilon_{e0}(\text{D}, V))\} &\simeq 1 - \beta(\varepsilon_{o1}(\text{D}, V) - \varepsilon_{e0}(\text{D}, V)) \\ \ln\{1 - w_o\beta(\varepsilon_{o1}(\text{D}, V) - \varepsilon_{e0}(\text{D}, V))\} &\simeq -w_o\beta(\varepsilon_{o1}(\text{D}, V) - \varepsilon_{e0}(\text{D}, V)) \end{aligned}$$

is used. Then, the partition function difference $\Xi_{\text{D-H}}(V_h, T)$ is

$$\begin{aligned} \Xi_{\text{D-H}}(V_h, T) &\simeq -\beta(\varepsilon_{e0}(\text{D}, V) - \varepsilon_{e0}(\text{H}, V)) \\ &\quad - w_o^{\text{D}}\beta(\varepsilon_{o1}(\text{D}, V) - \varepsilon_{e0}(\text{D}, V)) + w_o^{\text{H}}\beta(\varepsilon_{o1}(\text{H}, V) - \varepsilon_{e0}(\text{H}, V)) \end{aligned}$$

and the auxiliary function $\mathcal{H}(V_h; T)$ is

$$\begin{aligned} \mathcal{H}(V_h; T) &= -\frac{\partial}{\partial\beta}\Xi_{\text{D-H}}(V_h, T) \\ &\simeq c_{e0}^{(0)}\left(\frac{\hbar^2}{I_{\text{D}}} - \frac{\hbar^2}{I_{\text{H}}}\right) + c_{e0}^{(1)}V_h^{1/2}\left\{\left(\frac{\hbar^2}{I_{\text{D}}}\right)^{1/2} - \left(\frac{\hbar^2}{I_{\text{H}}}\right)^{1/2}\right\} \\ &\quad + w_o^{\text{D}}\left[\left(c_{o1}^{(0)} - c_{e0}^{(0)}\right)\frac{\hbar^2}{I_{\text{D}}} + \left(c_{o1}^{(1)} - c_{e0}^{(1)}\right)V_h^{1/2}\left(\frac{\hbar^2}{I_{\text{D}}}\right)^{1/2} + \left(c_{o1}^{(2)} - c_{e0}^{(2)}\right)V_h\right] \\ &\quad - w_o^{\text{H}}\left[\left(c_{o1}^{(0)} - c_{e0}^{(0)}\right)\frac{\hbar^2}{I_{\text{H}}} + \left(c_{o1}^{(1)} - c_{e0}^{(1)}\right)V_h^{1/2}\left(\frac{\hbar^2}{I_{\text{H}}}\right)^{1/2} + \left(c_{o1}^{(2)} - c_{e0}^{(2)}\right)V_h\right] \end{aligned}$$

In the double delta, $\Delta_{\text{D-H}}\Delta H = \mathcal{H}(V_h^{\text{GA}}; T) - \mathcal{H}(V_h^{\text{A}}; T)$, the term $c_{e0}^{(0)}$ is canceled out, and the leading terms are those of $c_{e0}^{(1)}$. By inserting the numerical values for the inertia moments, the statistical weights and the coefficients of the polynomial fits in (30), we get

$$\Delta_{\text{D-H}}\Delta H / \text{kJ/mol} \simeq -0.2313 \left\{ (V_h^{\text{GA}})^{1/2} - (V_h^{\text{G}})^{1/2} \right\} + 3.7 \times 10^{-4} (V_h^{\text{GA}} - V_h^{\text{G}})$$

Because $\left(\frac{\hbar^2}{I_{\text{D}}}\right)^{1/2} - \left(\frac{\hbar^2}{I_{\text{H}}}\right)^{1/2}$ is negative and $(c_{o1}^{(1)} - c_{e0}^{(1)})$ is positive, the auxiliary function $\mathcal{H}(V_h; T)$ has a negative slope as a function of V_h , and thus, $\Delta_{\text{D-H}}\Delta H$ becomes negative. With a little more complicated equation, the negative $\Delta_{\text{D-H}}\Delta S$ can be shown with a simple two-state model.

DISCUSSION AND REMARKS

Assuming only the change of the barrier height of the methyl internal rotation of the guest molecule caused by the encapsulation, we can qualitatively explain the experimental findings (2), (3), and (4) in the large isotope effects on the chemical equilibrium of the encapsulation reaction. The model gives us the correct order of magnitude of $\Delta_{\text{D-H}}\Delta H^{\text{VH}}$. Because the change of the barrier height of the methyl group is not simply related to the total binding of the encapsulation, the double delta, $\Delta_{\text{D-H}}^{\text{mod el}}\Delta H^{\text{VH}}$ and $\Delta_{\text{D-H}}^{\text{mod el}}\Delta S^{\text{VH}}$, are not necessarily correlated to the encapsulation equilibrium itself as the finding (4) describes. Thus, our simple model is consistent of four of the characteristics in Table 1. Besides, the increase of the rotational barrier of the end methyl groups is also congruent with a picture of the methyl CH non-covalently interacting with the π electrons of the phenyl groups of the host cage.

But, with the current simple model, an apparently large change ΔV_h by the encapsulation is required for $\Delta_{\text{D-H}}^{\text{mod el}}\Delta H^{\text{VH}}$. If the methyl rotation is coupled with the main frame of the guest molecule, the real value of the barrier is reduced by a factor given in equation (28). The factor does differ not much from 1; the factor is not enough small to reduce the large ΔV_h to a reasonable value. Furthermore, $|\Delta_{\text{D-H}}^{\text{mod el}}\Delta S^{\text{VH}}|$ is too small compared with those in Table 1. So it is clear that more sophisticated low-frequency modes also contribute to the isotope effects of the encapsulation equilibrium. Those modes have to be influenced by the replacement of CH_3 with CD_3 . Three of the torsional modes of the whole guest molecule inside of the cage are the best candidates. The inertia moment of the long axis is not much changed by the deuteration, and it is partly taken into account through the factor in equation (28). The axes of other two torsional modes are perpendicular to the long axis, and the replacement of CH_3 with CD_3 may change their inertia moments more than that of the long axis, because the masses of the ends of the long molecules are changed. To assess the contribution from those modes, the guest specific calculations are required. In reality, inside of the cage, two methyl rotations and three torsional motions of the guest molecule are coupled. To correlate the numbers in

Table 1 with the theoretical values quantitatively, a little more sophisticated model studies specific to the guest molecule than the present one are required.

Although the quantitative explanation cannot be reached with the current model study, it is certain that the change of the barrier height of the methyl groups by the encapsulation is the key player of the observed large isotope effects. The dynamics and molecular interaction inside of the cage can be revealed by exploring the observed isotope effects.

Acknowledgement

The work was started when one of the authors (SI) was a special professor of Hiroshima University under the Special Coordination Funds for Promoting Science and Technology from MEXT, Japan in 2004-2008. He sincerely thanks Prof. M. Aida of Hiroshima University for giving him an opportunity to return to the research. The work is partially supported by the Grants-in-Aid for Science Research (No.17550012 and 20550018) of JSPS.

REFERENCES

- 1) T. Haino, K. Fukuda, H. Iwamoto, and S. Iwata, *in preparation* (2009).
- 2) K. -W. Chi, C. Addicott, Y. Kryschenko, and P. Stang, *J. Org. Chem.*, **69**, (2004) 964.
- 3) K. Kobayashi, Y. Yamada, M. Yamanaka, Y. Sei, and K. Yamaguchi, *J. Am. Chem. Soc.*, **126**, (2004) 13896.
- 4) T. Haino, M. Kobayashi, M. Chikaraishi, and Y. Fukazawa, *Chem. Commun.*, (2005) page 2321.
- 5) T. Haino, M. Kobayashi, and Y. Fukazawa, *Chemistry European J.*, **12**, (2006) 3310.
- 6) K. Fukuda, M. Kobayashi, T. Haino, and Y. Fukazawa In *The Spring Annual meeting of Chem. Soc. Japan*, (2007).
- 7) F. Mohamadi, N. Richards, W. Guida, R. Liskamp, M. Lipton, C. Caufield, G. Chang, T. Hendricksen, and W. Still, *J. Comp. Chem.*, **11**, (1990) 440.
- 8) Hobza, *Annu. Rep. Prog. Chem. Sec. C*, **100**, (2004) 3.
- 9) Y. -L Zhao, K. Houk, D. Rechavi, A. Scarso, and J. J. Rebek, *J. Amer. Chem. Soc.*, **126**, (2004) 11428.
- 10) K. Pitzer and Brewer, *Thermodynamics*, McGraw-Hill, 1961.
- 11) K. Pitzer, *J. Chem. Phys.*, **5**, (1937) 469.
- 12) K. Pitzer and W. Gwinn, *J. Chem. Phys.*, **10**, (1942) 428.
- 13) J. Li and K. Pitzer, *J. Phys. Che.*, **60**, (1956) 466.
- 14) H. Nielsen, *Phys. Rev.*, **40**, (1932) 445.